Nanoscale Systems for Optical Quantum Technologies

Grant Agreement No: 712721
Start Date: 1st October 2016 - Duration: 36 months

D1.2 Co-doped nanoparticles

Deliverable:	D1.2
Work package:	WP1 Nano-materials, optical micro-cavities and control systems
Task:	1.1 Y_2O_3 nanoparticles development
Lead beneficiary:	CNRS
Type:	Report
Dissemination level:	Public
Due date:	30 September 2017
Actual submission date:	22 September 2017
Author(s):	S. Liu , D. Serrano, P. Goldner (CNRS-CP)

This project has received funding from the European Union's Horizon 2020 research and innovation programme under grant agreement No 712721.

Version history

Version	Date	Author(s)	Description
V1	04/08/2017	D. Serrano (CNRS-CP)	Draft
V2	22/08/2017	D. Serrano, P. Goldner (CNRS-CP)	Revised draft
V3	20/09/2017	D. Serrano, P. Goldner, S. Liu (CNRS-CP),	Final draft, revised by A. Walther (ULUND)

Table of Contents

Deliverable Description

In this deliverable, we report on the synthesis and characterization of codoped Y_2O_3 nanoparticles. The choice of the codopants, praseodymium (Pr^{3+}) and neodymium (Nd^{3+}), follows the conclusions of deliverable D2.1 (Readout/qubit ion candidates). Furthermore, the suitability of this codoping for quantum information processing is discussed.

Introduction

One of the most pursued rare-earth based quantum computing approaches considers the possibility of employing a separate rare-earth ion to read out qubit states [1, 2]. In such a scheme, the fluorescence emission from this so-called 'readout ion' is used as a probe since the system can be prepared such that fluorescence is only emitted when the qubit is found at one of its two possible quantum states. This binary response is achieved by utilizing the permanent electric dipole-dipole interaction between the qubit ions and the readout ion with the aim of inducing a state selective out-of-resonance energy shift for the readout transition. For further details, an exhaustive description of the envisioned readout mechanism is given by Y. Yan et al. [3]. The choice of the rare-earth dopants acting as qubit and readout ions is not trivial since an important number of requirements are to be fulfilled by the pair. Long optical and hyperfine coherence times constitute the main criterion for a rare-earth dopant to be used as qubits. On the other hand, the choice of the readout ion relies on a high fluorescence yield since, at the single-ion level [2,3], the photon rate is capital for the readout transition to be efficiently detected [3,4]. Besides the mentioned criteria, additional aspects that should be taken into account include the strength of the permanent dipole-dipole interaction between the qubit ion and the readout ion [3,5], the need of avoiding readout ions presenting energy levels which are resonant with the qubit optical transition, and finally, the need of ensuring a negligible impact of possible energy transfer mechanisms on the readout scheme efficiency [5].

The 4f-4f transitions of the rare-earth ions present long optical population lifetimes (in the μs and ms ranges) leading to low emission rates and making them unsuitable for readout purposes. For this reason, investigations had strongly focused on the Ce^{3+} 5d transition (40 ns lifetime) as one of the very few options among the rare-earth series to play the role of readout ion. Nevertheless, the pairing of Ce^{3+} with Pr^{3+} and Eu^{3+} as qubit ions was investigated and found not to fully fulfill the previously mentioned criteria [5]. In this context, NanOQTech's approach of reducing the rare-earth lifetime in optical micro-cavities by means of Purcell effect (WP2) re-opens the choice of the readout ion to a much larger number of possibilities. In deliverable D2.1:*Readout/qubit ion candidates*, two codopings were concluded to be the most adapted for quantum computing purposes using rare-earth nanoparticles coupled to micro-cavities. These codopings are Pr^{3+}-Nd^{3+} and Eu^{3+}-Nd^{3+}, in which Nd^{3+} is proposed as readout ion for Pr^{3+} and Eu^{3+} based qubits.

Eligibility criteria

In order to confirm the absence of overlap between the Nd^{3+} transitions and the Pr^{3+} and Eu^{3+} transitions, one of the important eligibility criterion evocated above, the low temperature absorption spectrum of a singly doped Nd^{3+}:Y_2O_3 sample was recorded between 570 and 630 nm (Fig. 1). The Pr^{3+} and Eu^{3+} optical transitions used for qubit initialization and manipulation are found within this range, more precisely at 618.90 nm

($^3H_4 \rightarrow {}^1D_2$) and 580.88 nm ($^7F_0 \rightarrow {}^5D_0$) respectively (energy level diagram given in Annex, Supplementary Fig. 1). Thus, presence of Nd^{3+} absorptions at the mentioned wavelengths is highly undesired. As observed in Figure 1a, Nd^{3+} does present strong absorption peaks around 581 nm, coincident with the 580.88 nm Eu^{3+} qubit transition. In contrast, no Nd^{3+} absorption is observed at 618.90 nm (Fig. 1b), corresponding to the Pr^{3+} qubit wavelength. From this analysis, a choice is taken between the preliminary proposed codopings. Thus, the Nd^{3+}-Eu^{3+} codoping is discarded for presenting qubit ion – readout ion transition overlap while the Pr^{3+}-Nd^{3+} codoping is confirmed as a good candidate and further pursued.

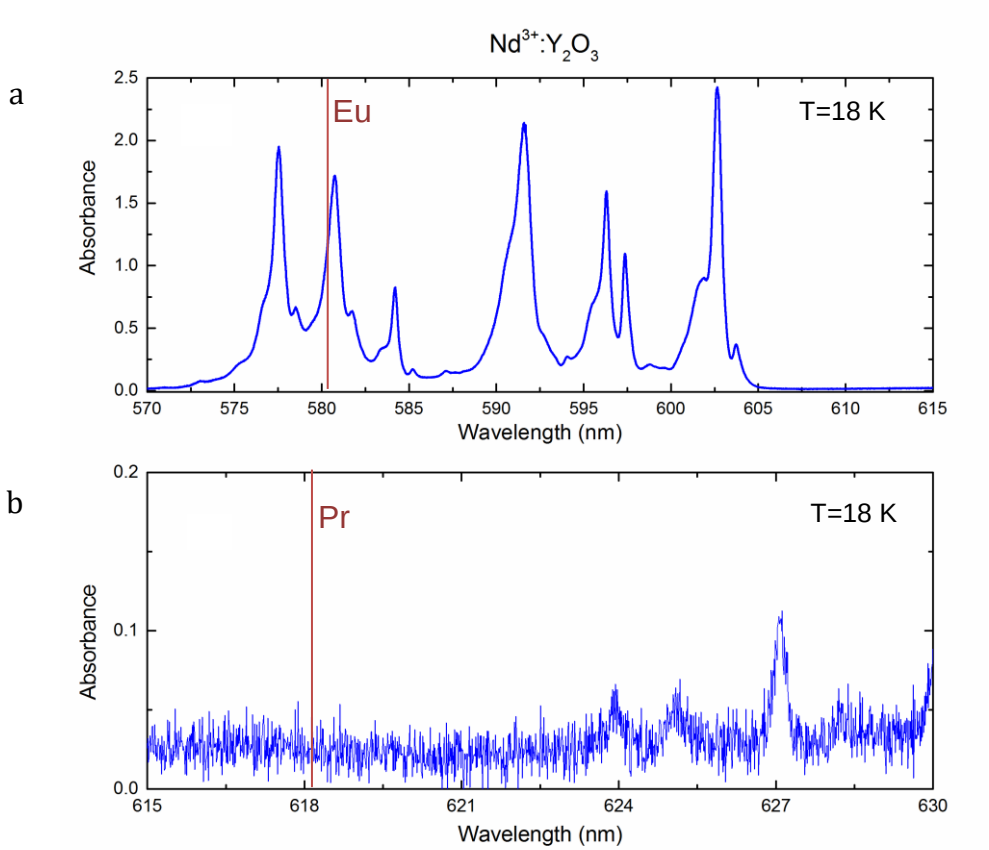

Figure 1: Low temperature absorption spectrum of Nd^{3+} in Y_2O_3 transparent ceramics (0.4%at.). (a) In the 570 - 615 nm spectral range, the observed absorption peaks correspond to the $^4I_{9/2} \rightarrow {}^2G_{7/2}$ and $^4I_{9/2} \rightarrow {}^4G_{5/2}$ Nd^{3+} transitions. (b) Only weak absorption transitions are observed in the 615-630 nm range, associated to the $^4I_{9/2} \rightarrow {}^2H_{11/2}$ absorptions. The spectra were recorded with a Cary 6000i UV–Vis–NIR spectrophotometer.

Pr^{3+}- Nd^{3+}:Y_2O_3 nanoparticles synthesis

Monodispersed Pr^{3+}-Nd^{3+} codoped Y_2O_3 spherical particles were synthetized by homogeneous precipitation [6]. $Y(NO_3)_3.xH_2O$ (99.99% pure, Alfa Aesar[1]), $Nd(NO_3)_3.xH_2O$ (99.99% pure, Alfa Aesar[1]) and $Pr(NO_3)_3.6H_2O$ (99.999% pure, Alfa Aesar) were used as starting materials. The same concentration was used for both Pr^{3+} and Nd^{3+}codopants, equals to 0.1 at.%. In a typical synthesis, an appropriate amount of urea ($CO(NH_2)_2$, 99%

[1] The exact water amount in the precursor is not stated by Alfa Aesar but estimated between 5 and 6.

pure, Sigma) was dissolved in a mixed Pr,Nd/Y aqueous nitrate solutions to make a total solution volume of 800 ml. The concentrations were 0.3 mol.l^{-1} for urea and 7.5 mmol.l^{-1} for metals (Pr^{3+}, Nd^{3+} and Y^{3+}). The mixed solutions were heated at 85 °C for 24 h in a Teflon reactor. After this reaction time, the final suspensions were cooled to ambient conditions and the colloidal particles collected via centrifugation. The wet precipitates were washed with distilled water once to remove the byproducts, then rinsed twice with absolute ethanol, and dried at 80 °C for 24 h to yield a Pr^{3+}, Nd^{3+}: $Y(OH)CO_3$ (YOC) powder. The Pr^{3+}, Nd^{3+}:Y_2O_3 nanoparticles were obtained by calcination of these original YOC powders at 1200 °C for 6 h under air atmosphere with a heating rate of 3 °C min^{-1}.

A scheme of this synthesis process is presented as follows:

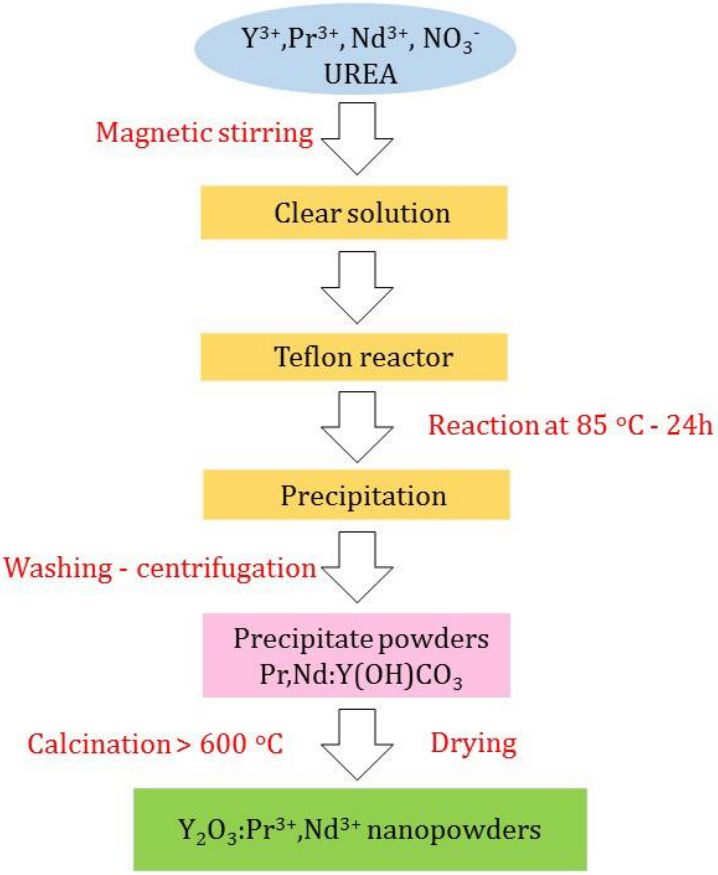

Structural and morphological characterizations

The particles' morphology, size and dispersion were determined by scanning electron microscopy (SEM) (Fig. 2). X-ray diffraction (XRD) analysis was used to confirm the crystalline phase of the particles. As displayed in Figure 3, the observed peaks are characteristic from the body-centered cubic (bcc) Y_2O_3 structure (Ia-3 space group) given in the standard reference. No additional peaks corresponding to parasitic phases were found.

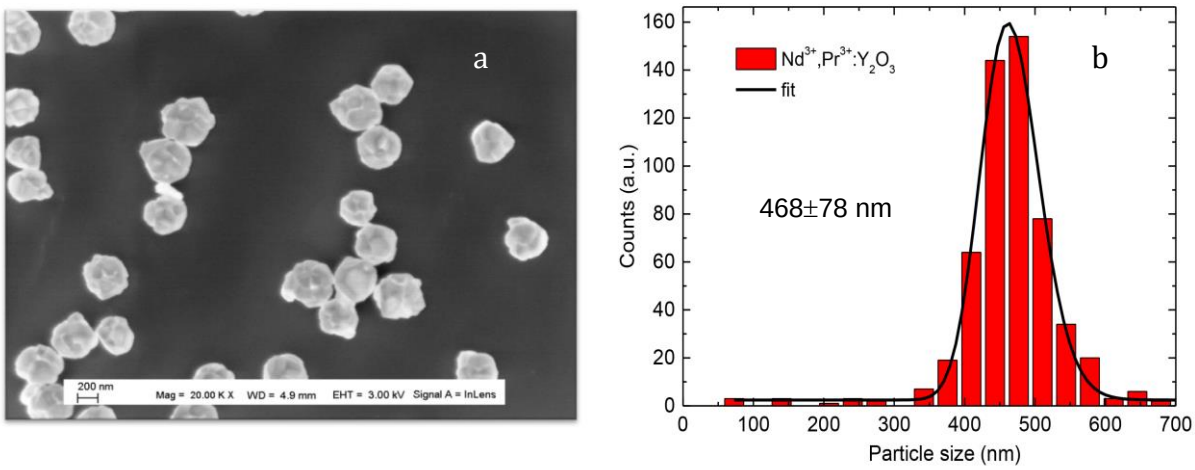

Figure 2: (a) SEM image of the 0.1%Pr^{3+}-0.1%Nd^{3+}:Y_2O_3 codoped particles. (b) Size distribution histogram revealing an average particle diameter of 468±78 nm.

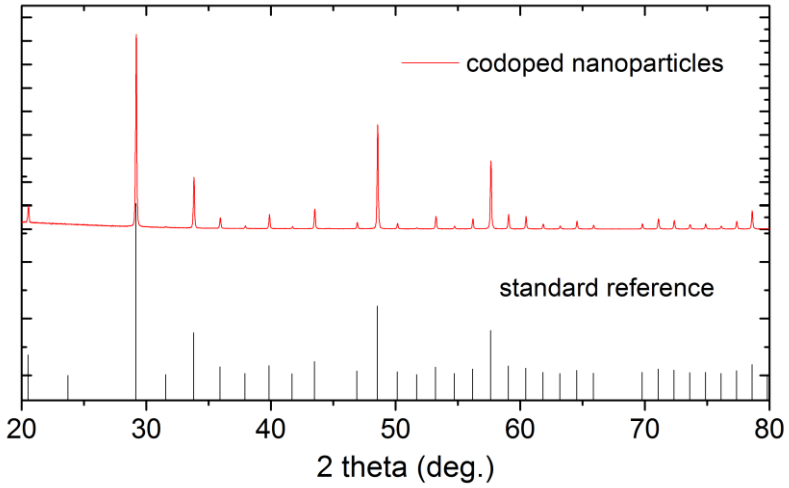

Figure 3: XRD pattern of the 0.1%Pr^{3+}-0.1%Nd^{3+}:Y_2O_3 codoped particles compared to the standard Y_2O_3 reference.

Spectroscopic investigations

Cathodoluminescence (CL) spectroscopy was performed on a single nanoparticle by using a 10 kV electron beam produced in a JEOL 7001F scanning electron microscope equipped with a field effect gun. The emitted light was collected by a parabolic mirror and focused with mirror optics on a monochromator (Horiba Jobin Yvon TRIAX550). The CL spectra were recorded with a UV-enhanced silicon CCD camera. Photoluminescence (PL) spectra were carried out with an optical parametric oscillator (OPO) pumped by the third harmonic (355 nm) of a Nd:YAG laser as excitation source. The light emitted by the sample was dispersed by a spectrometer (Acton SP2300) and detected by a cooled down CCD camera (Princeton Instruments). Fluorescence decay curves were detected with a photomultiplier tube (PMT).

The CL spectrum of a single Y_2O_3:0.1%Pr^{3+}-0.1%Nd^{3+} nanoparticle is displayed in Figure 4. Emission peaks between 600 nm and 750 nm can be recognized as due to the Pr^{3+} dopants, in particular to $^1D_2$ emissions [7]. On the other hand, the emission peaks between

850 and 1000 nm were identified as due to Nd^{3+}:$^4F_{3/2}$→$^4I_{9/2}$ emissions demonstrating the presence of both dopants in the particle. PL spectra obtained under selective Pr^{3+} and Nd^{3+} excitation, displayed in Figure 5, are in agreement with the CL results, confirming the peak assignment.

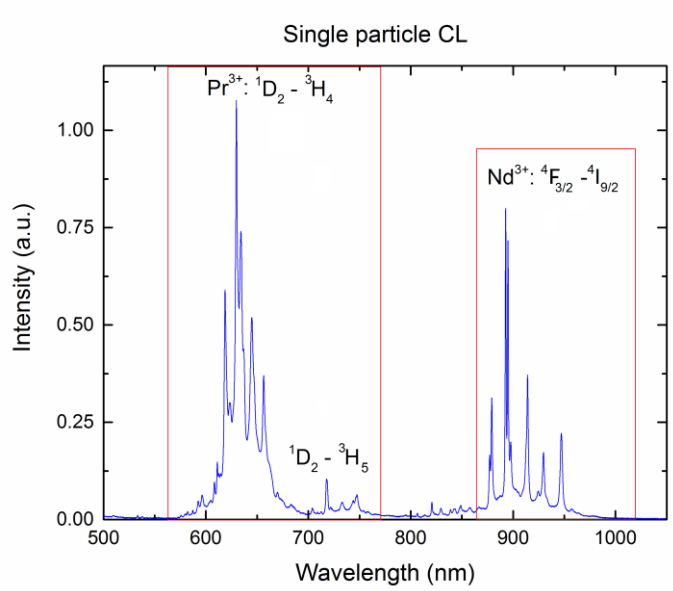

Figure 4: Room temperature (RT) cathodoluminescence (CL) spectrum of a single Y_2O_3:0.1%Pr^{3+}-0.1%Nd^{3+} nanoparticle.

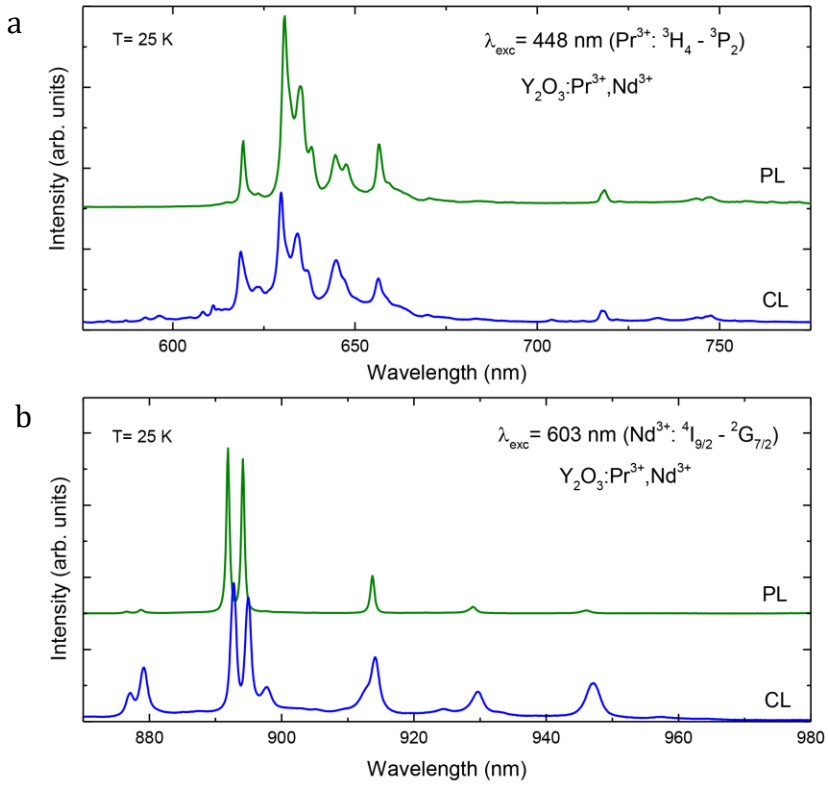

Figure 5: (a) Low temperature emission spectrum of Pr^{3+} obtained under selective Pr^{3+} excitation at 448 nm compared to room temperature CL spectrum (b) Low temperature Nd^{3+} emission spectrum obtained under selective Nd^{3+} excitation at 603 nm compared to room temperature CL spectrum. Small shifts of the lines between CL and PL are attributed to the different temperatures used in the experiments.

Energy transfer

Rare-earth ions are well-known for presenting multiple energy transfer paths [9]. These energy transfer paths are actively investigated as they can be exploited in benefit of numerous applications [10]. In contrast, energy transfers constitute a detrimental loss mechanism for quantum information applications [5]. The occurrence of efficient energy transfer mechanisms from the readout ion towards the qubit ion has two main negative effects. First, it provokes a decrease in fluorescence yield for the readout ion since energy transfer constitutes a non-radiative relaxation path, and secondly, the quantum information encoded in the qubit ion is lost when this one becomes the energy transfer acceptor. The other way around, when the energy transfer takes place from the qubit ion to the readout ion leads to uncontrolled fluorescence emission as well as the previously mentioned loss of quantum information. Despite this, the simple existence of energy transfer paths between a qubit ion and a readout ion is not enough in itself to discard a rare-earth codoping since it is the efficiency of the energy transfer mechanism which is critical and determines their effective impact on quantum computing schemes [5].

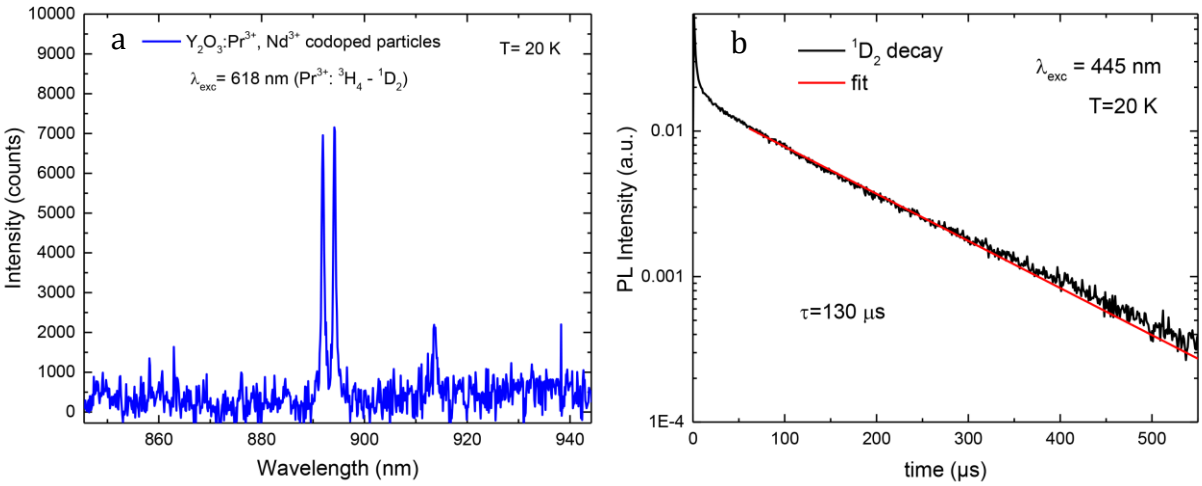

Figure 6: (a) Nd^{3+} emission obtained under selective Pr^{3+} excitation evidencing the occurrence of energy transfer from Pr^{3+}($^1D_2$) to Nd^{3+}. Low temperature Pr^{3+} $^1D_2$ fluorescence decay showing a time constant of 130 µs.

Evidence of energy transfer from Pr^{3+} ($^1D_2$) to Nd^{3+} was found in the Pr^{3+}-Nd^{3+}:Y_2O_3 codoped particles by selectively exciting the Pr^{3+} $^1D_2$ level at 618 nm while monitoring the Nd^{3+} emissions at 892 and 894 nm (Fig. 6a). The analysis of the energy level diagram (Suppl. Figure 1 in Annex) indicates that the Pr^{3+}:$^1D_2$→$^3H_6$; Nd^{3+}:$^4I_{9/2}$→$^4F_{5/2}$ cross-relaxation, responsible for the observed energy transfer, is the most prominent energy transfer path which can be expected for Pr^{3+}-Nd^{3+} pairs. The efficiency of the mechanism appears however to be low. The Nd^{3+} signal obtained after energy transfer from Pr^{3+} is very weak as it can be judged from the signal to noise ratio in Fig. 6a. In particular, the Nd^{3+} emission is three orders of magnitude weaker than signal obtained under direct Nd^{3+} excitation at 603 nm. Furthermore, no clear fluorescence lifetime quenching is observed for the $^1D_2$ level (Fig. 6b). The $^1D_2$ decay time was measured to 130 µs in agreement with values reported in literature for the same Pr^{3+} concentration in Y_2O_3 [7]. Further investigations are required to fully determine the impact of the observed energy transfer on the proposed readout mechanism. Nevertheless, this preliminary investigation points

to a low energy transfer efficiency which can be further limited by decreasing the doping concentration. The energy transfer efficiency is highly depending on the distance between ions (R^{-6}) [11] and therefore on the doping rate. At concentrations typically used for quantum information processing (~hundreds of ppm), the observed energy transfer mechanism can be expected to be extremely weak or even negligible.

Conclusion

Pr^{3+}-Nd^{3+} codoped Y_2O_3 nanoparticles were synthesized by homogeneous precipitation following the conclusions given in deliverable D2.1 (qubit/readout ions). The series of characterizations carried out confirmed the structural and spectroscopic features expected for the material. Single-particle cathodoluminescence was used to verify the homogeneous distribution of the codoping, with both codopants being present in a single particle. The occurrence of energy transfer from Pr^{3+} to Nd^{3+}, a detrimental mechanism for the readout scheme, was evidenced. The transfer efficiency was however concluded to be low and possibly negligible at concentrations typically used for quantum information processing. Next steps include the production of codoped particles with concentrations in the ppm range.

Bibliography

[1] A. Walther, "D2.1:Readout/qubit ion candidates". (March, 2017).
[2] J. H. Wesenberg, K. Moelmer, L. Rippe, S. Kröll, "Scalable designs for quantum computing with rare-earth-ion-doped crystals", *Phys. Rev. A* **75**, 012304 (2007).
[3] Y. Yan, J. Karlsson, L. Rippe, A. Walther, D. Serrano, D. Lindgren, M. E. Pistol, S. Kröll, P. Goldner, L. Zheng and J. Xu, "Measurement of linewidths and permanent electric dipole moment change of the Ce 4 f-5 d transition in Y_2SiO_5 for qubit readout scheme in rare-earth ion based quantum computing", *Phys. Rev. B* **87** (18), 184205 (2013).
[4] R. Kolesov, K. Xia, R. Reuter, R. Stöhr, A. Zappe, J. Meijer, P.R. Hemmer and J. Wrachtrup, "Optical detection of a single rare-earth ion in a crystal", *Nat. Commun.* **3**, 1029 (2011).
[5] D. Serrano, Y. Yan, J. Karlsson, L. Rippe, A. Walther, S. Kröll, A. Ferrier, P. Goldner, "Impact of the ion-ion energy transfer on quantum computing schemes in rare-earth doped solids", *J. Lum.* **151**, 93 (2014).
[6] K.O. Lima, R.R. Gonçalves, D. Giaume, A. Ferrier, P. Goldner," Influence of defects in sub-Å optical linewidhts in Eu^{3+}:Y_2O_3 nanoparticles", *J. Lum.* **168,** 276 (2015).
[7] Y. Guyot, R. Moncorgé, L.D. Merkle, A. Pinto, B. McIntosh, H. Verdun, "Luminescence properties of Y_20_3 single crystals doped with Pr^{3+} or Tm^{3+} and codoped with Yb^{3+}, Tb^{3+} or Ho^{3+} ions", *Opt. Mater.* **5**, 127 (1996).
[8] B. M. Walsh, J. M. MacMahon, W. C. Edwards, N. P. Barnes, R. W. Equall, R. L. Hutcheson, "Spectroscopic characterization of Nd:Y_2O_3: application toward a differential absorption lidar system for remote sensing of ozone". *J. Opt. Soc. Am. B* **19** (12) (2002).
[9] L. G. van Uitert,"Characterization of energy transfer interaction between rare-earth ions", *J. Electrochem. Soc.* **114** (10) (1967).
[10] X. Liu, J. Qiu, "Recent advances in energy transfer in bulk and nanoscale luminescent materials: from spectroscopy to applications", *Chem. Soc. Rev.* **44**, 8741 (2015).
[11] D.L. Dexter,"A theory of sensitized luminescence in solids", *J. Chem. Phys.* **21**, 836 (1953).

Annex: Energy level scheme

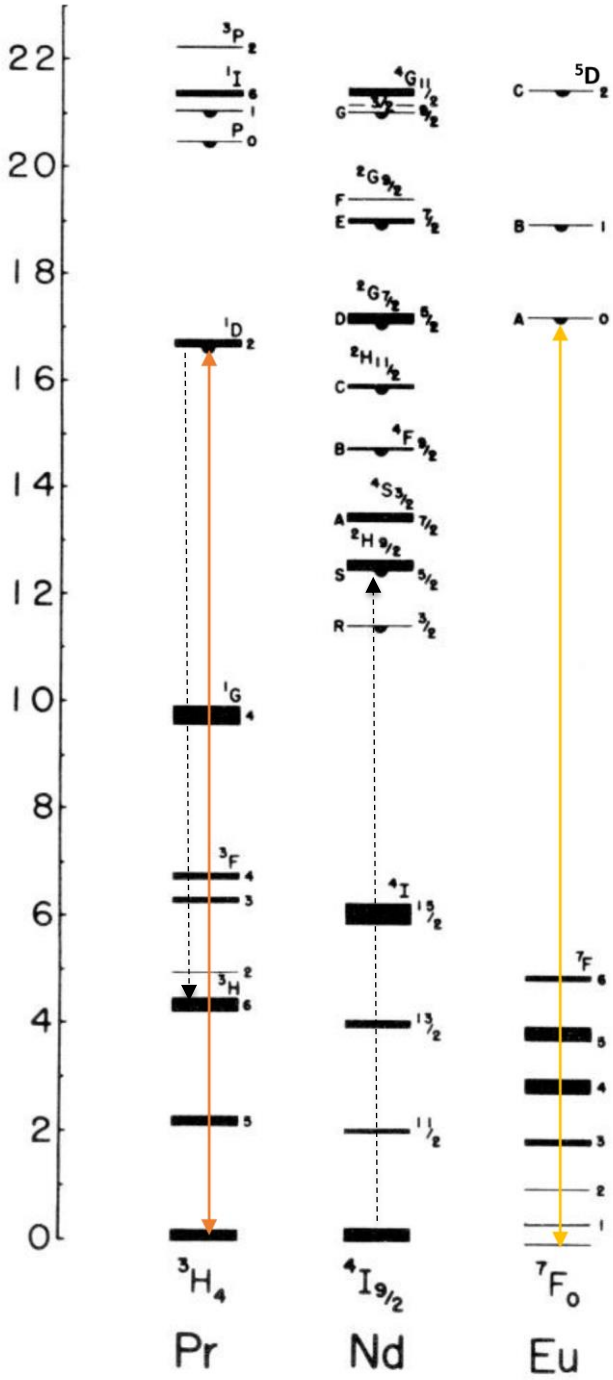

Supplementary Figure 1: Energy level diagram of the ions under discussion. Straight arrows indicate the Pr^{3+} and Eu^{3+} qubit optical transitions. The experimentally observed cross-relaxation path is highlighted by discontinuous arrows.